MMSE-ZF RECEIVER AND BLIND ADAPTATION FOR MULTIRATE CDMA

Irfan Ghauri and Dirk T. M. Slock

Institut Eurécom *

2229-Route des Crêtes, B.P. 193, F-06904 Sophia–Antipolis CEDEX, France

E-mail: {ghauri, slock}@eurecom.fr

ABSTRACT

We consider multirate users in a DS-CDMA system operating in an asynchronous fashion in a multipath environment. Oversampling w.r.t. the chip rate is applied to the cyclostationary received signal and multi-sensor reception is considered, leading to a linear multichannel model. Channels for different users are considered to be FIR and of possibly different lengths, depending upon their processing gains. We consider an individualized linear MMSE-ZF or projection receiver for a given user, exploiting its spreading sequence and timing information. Due to the periodically varying nature of the symbol spreading sequences for fast users in a multirate setup, the symbol rate cyclostationarity no longer holds for all users. However, the multiuser signal is still cyclostationary with the period P, where P is the processing gain at the slowest rate. A u_k times faster user k behaves as if it were a linear combination of u_k users at the slowest rate. The problem boils down to classical multiuser detection with time-varying interference cancelling filters for faster users. The processing is time-invariant, however, when performed at rate P. In that case, u_k symbols for the kth user get estimated simultaneously through u_k parallel receivers. We discuss the blind estimation of the channels, required for determining the linear multirate receivers, via a constrained minimum output energy approach.

I. INTRODUCTION

Multirate transmission is an alternative to multicode transmission for achieving high data rates in DS-CDMA networks [1]. The latter technique employs several channelization codes from a given set of spreading sequences of the same length to transmit data. Hence the input symbol stream at a high rate is demultiplexed and is spread by different spreading sequences to achieve greater capacity through parallel transmission. The disadvantage of such an approach is that large fluctuations in the received signal envelope impose a severe constraint on the power amplifier at the receiver, which needs to operate within a large dynamic range. Multirate transmission has therefore been preferred in the third generation WCDMA proposal [1], for high rate communications, especially in the case of small delay spreads (indoor and pedestrain channels). The processing gains for different users are a function of their transmission rates. This, however, does not mean that the faster users are penalized in terms of the bit energy to noise power ratio, and the chip energy is therefore larger for high rate users, leading to the same E_b/N_0 for all users.

Naturally, for a given channel, the intersymbol interference (ISI) can be significantly large for a faster user. The effect of the increased ISI is however reduced if periodically varying spreading sequences are employed, so that the spreading sequence cyclically varies at a rate of $1/u_k$, where $u_k = P/P_k$, and P is the cyclostationarity period (also the processing gain of the slowest possible rate, e.g., $P = 256$ in the UMTS WCDMA proposal). Nevertheless, some kind of ISI cancellation is likely to result in improved performance.

The purpose of this paper is to give insight into the multirate problem from a signal processing standpoint while presenting the MMSE-ZF [2] or projection receiver [3], taking into account the periodically time varying (PTV) nature of the spreading sequences. A description of multirate systems has also been given in [4].

The receiver presented in this paper is a per user (decentralized) receiver in the sense that its estimation requires the knowledge of the desired user's spreading sequence and timing information along with the second order statistics of the received signal. We show that a u_k times faster users can be split into u_k slower users, and the treatment of the problem remains the same as for lowest rate users. Identifiablity issues are addressed and the implications of such an approach are discussed.

II. MULTIRATE DS-CDMA

Fig. 1 shows the discretized model for a $u_k = 2$ times faster user in the system ($P_k = P/2$), with P the basic processing gain of the system. $\boldsymbol{h}_k$ represents the chip-rate channel for the kth user, and $\mathcal{T}(h_k)$ is the corresponding channel convolution matrix. The overall system therefore depicts spreading of successive symbols $a_k(n)$ by spreading sequences $\boldsymbol{c}_k$, which are later passed through $\boldsymbol{h}_k$, the discrete-time chip rate channel. It can be seen that for a user transmitting u_k times faster than the slowest rate, the block diagonal spreading matrices $\mathcal{T}(\boldsymbol{c}_k)$ have periodically varying (with period u_k) vector elements on the diagonal. Due to the *i.i.d.* nature of the input data sequence, $a_k(n)$, this user can be viewed as u_k cyclostationary users with modified spreading sequences shown in the figure with zeros padded at the end.

This representation of faster users in a multirate system motivates the design of periodically time variant filters or yet better,

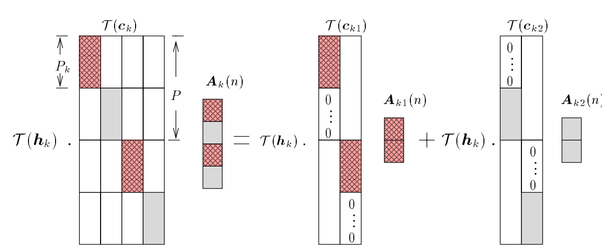

Figure 1. Representation of a high-rate user as two slow-rate users, $P_k = P/2$.

*Eurecom's research is partially supported by its industrial partners: Ascom, Cégétel, France Télécom, Hitachi, IBM France, Motorola, Swisscom, Texas Instruments, and Thomson CSF

independent parallel receivers for the successive symbols of a certain faster user. The advantage of the split-up approach is that the estimation of these filters is independent of each other, exactly as if they were independent users. If the system has $K^{'}$ concurrent users transmitting at different rates, then let us denote by K, where, $K = \sum_{k=1}^{K^{'}} u_k$, the modified number of the basic rate users in the system. In the following, we shall consider this slowest rate representation of a multirate system with K effective users, and a processing gain, P, and concentrate on the detection of data symbols for the kth user, which might be a sub-user of a higher rate.

III. MULTIUSER DATA MODEL

Fig. 2 shows the baseband signal model. The K users are assumed to transmit linearly modulated signals over a linear multipath channel with additive Gaussian noise. It is assumed that the receiver employs M sensors to receive the mixture of signals from all users. The receiver front-end is an anti-aliasing low-pass filter. The continuous-time signal received at the mth sensor can be written in baseband notation as

$$y^m(t) = \sum_{k=1}^{K} \sum_{n} a_k(n) g_k^m(t - nT) + v^m(t), \qquad (1)$$

where the $a_k(n)$ are the transmitted symbols from user k, T is the common symbol period, $g_k^m(t)$ is the overall channel impulse response (including the spreading sequence, and the transmit and receive filters) for the kth user's signal at the mth sensor, and $\{v^m(t)\}$ is the complex circularly symmetric AWGN with power spectral density N_0. Assuming the $\{a_k(n)\}$ and $\{v^m(t)\}$ to be jointly wide-sense stationary, the process $\{y^m(t)\}$ is wide-sense cyclostationary with period T. The overall channel impulse response $g_k^m(t)$, is the convolution of the spreading code c_k and $h_k^m(t)$, itself the convolution of the chip pulse shape, the receiver filter, and the actual channel representing the multipath environment. This can be expressed as

$$g_k^m(t) = \sum_{p=0}^{P-1} c_k(p) h_k^m(t - pT_c), \qquad (2)$$

where T_c is the chip duration. The symbol and chip periods are related through the processing gain/spreading factor P: $T = PT_c$. S/P in fig. 2 denotes serial-to-parallel conversion (vectorization) with downsampling of a factor J. Sampling the received signal at J (oversampling factor) times the chip rate, we obtain the wide-sense stationary $PJ \times 1$ vector signal $\boldsymbol{y}^m(n)$ at

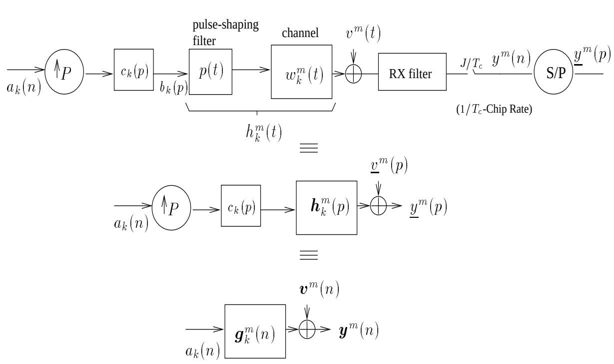

Figure 2. Signal model in continuous and discrete time, showing only the contribution from one user.

the symbol rate. It is to be noted that the oversampling aspect (with respect to the symbol rate) is inherent to DS-CDMA systems by their very nature, due to the large (extra) bandwidth and the need to acquire chip-level resolution. This aspect directly translates into temporal diversity and explains the interference cancellation capability of these systems.

We consider the channel delay spread between the kth user and all of the M sensors to be of length $l_k T_c$. Let $n_k \in \{0, 1, \cdots P-1\}$ be the chip-delay index for the kth user: $\boldsymbol{h}_k^m(n_k)$ is the first non-zero $J \times 1$ chip-rate sample of $\boldsymbol{h}_k^m(p)$. Let us denote by N_k, the FIR duration of $g_k^m(t)$ in symbol periods. It is a function of l_k, n_k, and P. We nominate the user 1 as the user of interest and assume that $n_1 = 0$ (synchronization to user 1). The symbol sequences for other users are relabeled (delayed or advanced), so that their relative delay with respect to user 1 falls in $[0, T)$.

Let $N = \sum_{k=1}^{K} N_k$. The vectorized oversampled signals at M sensors lead to a discrete-time $PMJ \times 1$ vector signal at the symbol rate that can be expressed as

$$\begin{aligned} \boldsymbol{y}(n) &= \sum_{k=1}^{K} \sum_{i=0}^{N_k-1} \boldsymbol{g}_k(i) a_k(n-i) + \boldsymbol{v}(n) \\ &= \sum_{k=1}^{K} \boldsymbol{G}_{k,N_k} A_{k,N_k}(n) + \boldsymbol{v}(n) = \boldsymbol{G}_N \boldsymbol{A}_N(n) + \boldsymbol{v}(n), \end{aligned} \qquad (3)$$

$$\boldsymbol{y}(n) = \begin{bmatrix} \boldsymbol{y}_1(n) \\ \vdots \\ \boldsymbol{y}_P(n) \end{bmatrix}, \boldsymbol{y}_p(n) = \begin{bmatrix} \boldsymbol{y}_p^1(n) \\ \vdots \\ \boldsymbol{y}_p^M(n) \end{bmatrix}, \boldsymbol{y}_p^m(n) = \begin{bmatrix} y_{p,1}^m(n) \\ \vdots \\ y_{p,J}^m(n) \end{bmatrix}$$

$$\begin{aligned} \boldsymbol{G}_{k,N_k} &= [\boldsymbol{g}_k(N_k-1) \ldots \boldsymbol{g}_k(0)] \ , \\ \boldsymbol{G}_N &= [\boldsymbol{G}_{1,N_1} \ldots \boldsymbol{G}_{K,N_K}] \\ A_{k,N_k}(n) &= [a_k(n-N_k+1) \ldots a_k(n)]^T \ , \\ \boldsymbol{A}_N(n) &= \left[A_{1,N_1}^T(n) \ldots A_{K,N_K}^T(n)\right]^T , \end{aligned} \qquad (4)$$

and the superscript ^{T} denotes transpose. For the user of interest (user 1), $\boldsymbol{g}_1(i) = (\boldsymbol{C}_1(i) \otimes I_{MJ})\, \boldsymbol{h}_1$, where, $\boldsymbol{h}_1$ is the $l_1 MJ \times 1$ propagation channel vector given by

$$\boldsymbol{h}_1 = \begin{bmatrix} \boldsymbol{h}_{1,1} \\ \vdots \\ \boldsymbol{h}_{1,l_1} \end{bmatrix}, \boldsymbol{h}_{1,l} = \begin{bmatrix} \boldsymbol{h}_{1,l}^1 \\ \vdots \\ \boldsymbol{h}_{1,l}^M \end{bmatrix}, \boldsymbol{h}_{1,l}^m = \begin{bmatrix} h_{1,l}^m(1) \\ \vdots \\ h_{1,l}^m(J) \end{bmatrix} ,$$

$\otimes$ denotes the Kronecker product, and the Toeplitz matrices $\boldsymbol{C}_1(i)$ are shown in fig. 3, where the band consists of the spreading code $(c_0 \cdots c_{P-1})^T$ shifted successively to the right and down by one position. For the interfering users, we have a similar setup except that owing to asynchrony, the band in fig. 3 is shifted down n_k chip periods and is no longer coincident

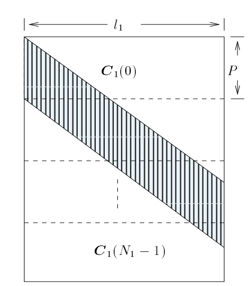

Figure 3. The Code Convolution Matrix $\boldsymbol{C}_1$.

with the top left edge of the box. We denote by $\boldsymbol{C}_1$, the concatenation of the code matrices given above for user 1: $\boldsymbol{C}_1 = [\boldsymbol{C}_1^T(0)\cdots\boldsymbol{C}_1^T(N_1-1)]^T$.

It is clear that the signal model above addresses a multiuser setup suitable for joint interference cancellation provided the timing information and spreading codes of all sources are available. As we shall see in the following, it is possible to decompose the problem into single user ones, thus making the implementation suitable for decentralized applications such as at mobile terminals or as a suboptimal processing or initialization stage at the base station. To this end, let us stack L successive $\boldsymbol{y}(n)$ vectors in a super vector

$$\boldsymbol{Y}_L(n)=\mathcal{T}_L(\boldsymbol{G}_N)\boldsymbol{A}_{N+K(L-1)}(n)+\boldsymbol{V}_L(n), \qquad (5)$$

where, $\mathcal{T}_L(\boldsymbol{G}_N) = [\mathcal{T}_L(\boldsymbol{G}_{1,N_1})\cdots\mathcal{T}_L(\boldsymbol{G}_{K,N_K})]$, and $\mathcal{T}_L(\boldsymbol{x})$ is a banded block Toeplitz matrix with L block rows and $\left[\boldsymbol{x} \quad \boldsymbol{0}_{p\times(L-1)}\right]$ as first block row (p is the number of rows in $\boldsymbol{x}$), and $\boldsymbol{A}_{N+K(L-1)}(n)$ is the concatenation of user data vectors ordered as $\left[A_{1,N_1+L-1}^T(n), A_{2,N_2+L-1}^T(n)\cdots A_{K,N_K+L-1}^T(n)\right]^T$. We shall refer to $\mathcal{T}_L(\boldsymbol{G}_{k,N_k})$ as the channel convolution matrix for the kth user. Consider the noiseless received signal shown in

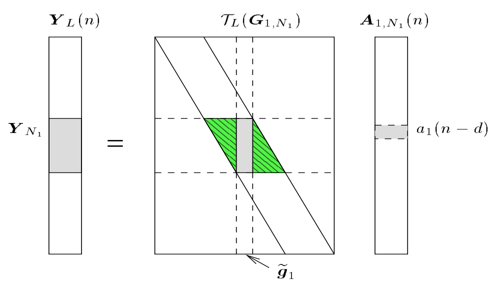

Figure 4. ISI for the desired user.

fig. 4 for the contribution of user 1, from which the following observations can be made. Due to the limited delay spread, the effect of a particular symbol, $a_1(n-d)$, influences N_1 symbol periods, rendering the channel a moving average (MA) process of order N_1-1 [5]. We are interested in estimating the symbol $a_1(n-d)$ from the received data vector $\boldsymbol{Y}_L(n)$. One can notice that $a_1(n-d)$ appears in the portion $\boldsymbol{Y}_{N_1}$ of $\boldsymbol{Y}_L(n)$. The shaded triangles constitute the ISI, i.e., the effect of neighboring symbols on $\boldsymbol{Y}_{N_1}$. The contributions from the other (interfering) users to the received data vector have a similar structure. Note that to handle ISI and MAI, it may be advantageous to consider the longer received data vector $\boldsymbol{Y}_L(n)$.

IV. THE MMSE-ZF RECEIVER

It was shown in [2], that the MMSE-ZF receiver could be obtained by a proper implementation of the unbiased minimum output energy [1] (MOE) criterion. We shall refer to [2] for details while mentioning that the MMSE-ZF receiver can be implemented in the generalized sidelobe canceler (GSC) [6] fashion as in the following.

Let us denote by

$$\boldsymbol{T}_1 = \begin{bmatrix}\boldsymbol{0} & \boldsymbol{C}_1^H & \boldsymbol{0}\end{bmatrix}\otimes \boldsymbol{I}_{MJ};\ \boldsymbol{T}_2 = \begin{bmatrix}\boldsymbol{I} & \boldsymbol{0} & \boldsymbol{0}\\ \boldsymbol{0} & \boldsymbol{C}_1^\perp & \boldsymbol{0}\\ \boldsymbol{0} & \boldsymbol{0} & \boldsymbol{I}\end{bmatrix}\otimes \boldsymbol{I}_{MJ}, \qquad (6)$$

[1] a derivative of the minimum variance distortionless response (MVDR) method, and a particular instance of the linearly constrained minimum-variance (LCMV) criterion

the partial signature of the desired user and its orthogonal complement employed, respectively, in the upper and lower branches of the GSC, as shown in fig. 5. $\boldsymbol{C}_1^{\perp H}$ is the orthogonal complement of $\boldsymbol{C}_1$, the tall code matrix given in section III ($\boldsymbol{C}_1^\perp\boldsymbol{C}_1 = \boldsymbol{0}$). Then, $\boldsymbol{C}_1^H\boldsymbol{Y}_{N_1} = \boldsymbol{T}_1\boldsymbol{Y}_L$ and the matrix $\boldsymbol{T}_2$ acts as a blocking transformation for all components of the signal of interest. Note that $P_{T_1^H} + P_{T_2^H} = \boldsymbol{I}$, where, P_X is the projection operator (projection on the column space of $\boldsymbol{X}$). Then the LCMV problem can be written as

$$\begin{aligned}&\min_{F:F^H T_1^H=(h_1^H h_1)^{-1}h_1^H} \boldsymbol{F}^H\boldsymbol{R}_{YY}^d\boldsymbol{F}\\ &= \min_{\substack{F\,:\,F^H T_1^H h_1 = 1\\ F^H T_1^H h_1^\perp = 0}} \boldsymbol{F}^H\boldsymbol{R}_{YY}^d\boldsymbol{F},\end{aligned} \qquad (7)$$

where, $\left[\boldsymbol{h}_1 \quad \boldsymbol{h}_1^\perp\right]$ is a square non-singular matrix, and $\boldsymbol{h}_1^H\boldsymbol{h}_1^\perp = \boldsymbol{0}$. Note that in the LCMV problem (GSC fomulation) there is a number of constraints to be satisfied. However, imposing the second set of constraints, namely $\boldsymbol{F}^H\boldsymbol{T}_1^H\boldsymbol{h}_1^\perp = 0$ has no consequence because the criterion automatically leads to their satisfaction once, $\mathrm{span}\{\boldsymbol{R}_{YY}^d\}\cap\mathrm{span}\{\boldsymbol{T}_1^H\} = \mathrm{span}\{\boldsymbol{T}_1^H\boldsymbol{h}_1\}$, i.e., when the intersection of the signal subspace and the subspace spanned by the columns of $\boldsymbol{T}_1^H$ is one dimensional.

The matrix $\boldsymbol{T}_1$ is nothing but a bank of correlators matched to the l_1 delayed multipath components of user 1's code sequence. Note that the main branch in fig. 5 by itself gives an unbiased response for the desired symbol, $a_1(n-d)$, and corresponds to the (normalized) coherent RAKE receiver. For the rest, we have an estimation problem, which can be solved in the least squares sense, for some matrix $\boldsymbol{Q}$. This interpretation of the GSC corresponds to the pre-combining (or pathwise) interference (ISI and MAI) canceling approach (see [7] and references therein).

The vector of estimation errors is given by

$$\boldsymbol{Z}(n) = [\boldsymbol{T}_1 - \boldsymbol{Q}\boldsymbol{T}_2]\,\boldsymbol{Y}_L(n). \qquad (8)$$

Since the goal is to minimize the estimation error variances, or in other words, estimate the interference term in the upper branch as closely as possible from $\boldsymbol{T}_2\boldsymbol{Y}_L(n)$, the interference cancellation problem settles down to minimization of the trace of the estimation error covariance matrix $\boldsymbol{R}_{ZZ}$ for a matrix filter $\boldsymbol{Q}$, which results in

$$\boldsymbol{Q} = \left(\boldsymbol{T}_1\boldsymbol{R}^d\boldsymbol{T}_2^H\right)\left(\boldsymbol{T}_2\boldsymbol{R}^d\boldsymbol{T}_2^H\right)^{-1}, \qquad (9)$$

and where, $\boldsymbol{R}^d$ is the noiseless (denoised) data covariance matrix, $\boldsymbol{R}_{YY}$, with the subscript removed for convenience. The output $\boldsymbol{Z}(n)$ can directly be processed by a multichannel matched filter to get the symbol estimate, $\hat{a}_1(n-d)$, the data for the user 1.

$$\begin{aligned}\hat{a}_1(n-d) &= \frac{1}{\widetilde{\boldsymbol{g}}_1^H\widetilde{\boldsymbol{g}}_1}\boldsymbol{F}^H\boldsymbol{Y}_L(n)\\ &= \frac{1}{\widetilde{\boldsymbol{g}}_1^H\widetilde{\boldsymbol{g}}_1}\boldsymbol{h}_1^H\left(\boldsymbol{T}_1-\boldsymbol{Q}\boldsymbol{T}_2\right)\boldsymbol{Y}_L(n)\end{aligned} \qquad (10)$$

The covariance matrix of the prediction errors is then given by

$$\boldsymbol{R}_{ZZ}=\boldsymbol{T}_1\boldsymbol{R}^d\boldsymbol{T}_1^H-\boldsymbol{T}_1\boldsymbol{R}^d\boldsymbol{T}_2^H\left(\boldsymbol{T}_2\boldsymbol{R}^d\boldsymbol{T}_2^H\right)^{-1}\boldsymbol{T}_2\boldsymbol{R}^d\boldsymbol{T}_1^H, \qquad (11)$$

From the above structure of the interference canceler, we observe that when $\boldsymbol{T}_1\left(\boldsymbol{Y}_L-\widetilde{\boldsymbol{g}}_1 a_1(n)\right)$ can be perfectly estimated from $\boldsymbol{T}_2\boldsymbol{Y}_L$, the matrix $\boldsymbol{R}_{ZZ}$ is rank-1 in the noiseless case! Using this fact, the desired user channel can be obtained (upto a scale factor) as the maximum eigenvector of the matrix $\boldsymbol{R}_{ZZ}$, since

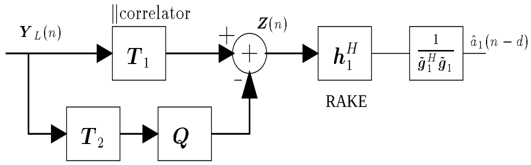

Figure 5. GSC implementation of the MMSE-ZF receiver.

$\boldsymbol{Z}(n) = (\boldsymbol{C}_1^H\boldsymbol{C}_1)\otimes\boldsymbol{I}_{MJ}\boldsymbol{h}_1\tilde{a}_1(n-d)$. It can further be shown easily that if $\boldsymbol{T}_2 = \boldsymbol{T}_1^{\perp}$, then

$$\boldsymbol{T}_1\boldsymbol{R}_{YY}^{-1}\boldsymbol{T}_1^H = \left(\boldsymbol{T}_1\boldsymbol{T}_1^H\right)\boldsymbol{R}_{ZZ}^{-1}\left(\boldsymbol{T}_1\boldsymbol{T}_1^H\right), \tag{12}$$

where, $\boldsymbol{R}_{ZZ}$ is given by (11), and $\boldsymbol{Q}$, given by (9), is optimized to minimize the estimation error variance. $\boldsymbol{R}^d$ replaces $\boldsymbol{R}_{YY}$ in the above developments. From this, we can obtain the propagation channel estimate for the desired user, $\hat{\boldsymbol{h}}_1$ as $\hat{\boldsymbol{h}}_1 = \mathrm{V}_{\max}\{\left(\boldsymbol{T}_1\boldsymbol{T}_1^H\right)^{-1}\boldsymbol{R}_{ZZ}\left(\boldsymbol{T}_1\boldsymbol{T}_1^H\right)^{-1}\}$. The above structure results in perfect interference cancellation (both ISI and MAI) in the noiseless case, the evidence of which is the rank-1 estimation error covariance matrix, and a consequent distortionless response for the desired user.

A. Identifiability Conditions for Blind MMSE-ZF Receiver

Continuing with the noiseless case, or with the denoised version of $\boldsymbol{R}_{YY}$, i.e., $\boldsymbol{R}_{YY}^d = \sigma_a^2\mathcal{T}_L(\boldsymbol{G}_N)\mathcal{T}_L^H(\boldsymbol{G}_N)$,

$$\min_{F:\,F^H\tilde{g}_1=1}\boldsymbol{F}^H\boldsymbol{R}_{YY}^d\boldsymbol{F} = \sigma_a^2, \quad \textit{iff} \quad \boldsymbol{F}^H\mathcal{T}_L(\boldsymbol{G}_N) = \boldsymbol{e}_d^T, \tag{13}$$

where, $\boldsymbol{e}_d = [0\cdots 0\ 1\ 0\cdots 0]^T$. This means that the zero-forcing condition must be satisfied. Hence, the unbiased MOE criterion corresponds to ZF in the noiseless case. This implies that $\mathrm{MOE}(\hat{\tilde{\boldsymbol{g}}}_1) < \sigma_a^2$ *if* $\hat{\tilde{\boldsymbol{g}}}_1 \not\sim \tilde{\boldsymbol{g}}_1$. We consider that:

(**i**). *FIR zero-forcing condition is satisfied*, and
(**ii**). $\mathrm{span}\{\mathcal{T}_L(\boldsymbol{G}_N)\}\cap\mathrm{span}\{\boldsymbol{T}_1^H\} = \mathrm{span}\{\boldsymbol{T}_1^H\boldsymbol{h}_1\}$.

The two step max/min problem boils down to

$$\max_{\hat{h}_1:\|\hat{h}_1\|=1}\hat{\boldsymbol{h}}_1^H\left(\boldsymbol{T}_1\boldsymbol{T}_1^H\right)^{-1}\boldsymbol{T}_1\mathcal{T}_L P^{\perp}_{\mathcal{T}_L^H T_2^H}\mathcal{T}_L^H\boldsymbol{T}_1^H\left(\boldsymbol{T}_1\boldsymbol{T}_1^H\right)^{-1}\hat{\boldsymbol{h}}_1, \tag{14}$$

where, $P_X^{\perp} = \boldsymbol{I}-\boldsymbol{X}(\boldsymbol{X}^H\boldsymbol{X})^{-1}\boldsymbol{X}^H$. Then identifiability implies that $\mathcal{T}_L P^{\perp}_{\mathcal{T}_L^H T_2^H}\mathcal{T}_L^H = \boldsymbol{T}_1^H\boldsymbol{h}_1\boldsymbol{h}_1^H\boldsymbol{T}_1 = \tilde{\boldsymbol{g}}_1\tilde{\boldsymbol{g}}_1^H$, or

$$P^{\perp}_{\mathcal{T}_L^H T_2^H}\mathcal{T}_L^H(\boldsymbol{G}_N) = P_{e_d^{'}}\mathcal{T}_L^H(\boldsymbol{G}_N), \tag{15}$$

Condition (i) above implies that $\boldsymbol{e}_d^{'}\in\mathrm{span}\{\mathcal{T}_L^H(\boldsymbol{G}_N)\}$. From condition (ii), since $\boldsymbol{T}_1^H\boldsymbol{h}_1 = \mathcal{T}_L(\boldsymbol{G}_N)\boldsymbol{e}_d$, we have

$$\begin{aligned}\mathrm{span}\{\mathcal{T}_L(\boldsymbol{G}_N)\boldsymbol{T}_2^H\} &= \mathrm{span}\{P_{e_d}^{\perp}\mathcal{T}_L^H(\boldsymbol{G}_N)\}\\ \mathrm{span}\{\mathcal{T}_L^H(\boldsymbol{G}_N)\} &= \mathrm{span}\{\mathcal{T}_L^H(\boldsymbol{G}_N)\boldsymbol{T}_2^H\}\oplus\mathrm{span}\{\boldsymbol{e}_d\}\end{aligned} \tag{16}$$

from which, $\mathcal{T}_L^H(\boldsymbol{G}_N) = P_{\mathcal{T}_L^H T_2^H}\mathcal{T}_L^H(\boldsymbol{G}_N) + P_{e_d}\mathcal{T}_L^H(\boldsymbol{G}_N)$, which is the same as (15).

B. Sufficiency of Conditions and Implications of the Split-up Scheme

We consider first the condition (**i**). Furthermore, in the following developments, we consider that $K < PMJ$, which is easily achievable with a small (e.g, 2) multiple sensor and/or oversampling factor. The effective number of channels is given by $(PMJ)_{\mathrm{eff}} = \mathrm{rank}\{\boldsymbol{G}_N\}$, where $\boldsymbol{G}_N$ is given in (3). Let $\mathbf{G}_1(z) = \sum_{n=0}^{N_1-1}\boldsymbol{g}_1(n)z^{-n}$ be the channel transfer function for user 1, with $\mathbf{G}(z) = [\mathbf{G}_1(z)\cdots\mathbf{G}_K(z)]$. Then let us assume the following:

(**a**). $\mathbf{G}(z)$ *is irreducible*, i.e., $\quad \mathrm{rank}\{\mathbf{G}(z)\} = K, \forall z.$
(**b**). $\mathbf{G}(z)$ *is column reduced*:

$$\mathrm{rank}\{[\boldsymbol{g}_1(N_1-1)\cdots\boldsymbol{g}_K(N_K-1)]\} = K.$$

Given that the above two conditions hold, the channel convolution matrix $\mathcal{T}_L(\boldsymbol{G}_N)$ is full rank w.p. 1, and the FIR length L required is given by,

$$L \geq \overline{L} = \left\lceil\frac{N-K}{(PMJ)_{\mathrm{eff}}-K}\right\rceil. \tag{17}$$

Note that condition (**a**) holds with probability 1 due to the quasi-orthogonality of spreading sequences. As for (**b**), it can be violated in certain limiting cases e.g., in the synchronous case where $\boldsymbol{g}_k(N_k-1)$'s contain very few non-zero elements. Under these circumstances, instantaneous (static) mixture of the sources [5] can null out some of the $\boldsymbol{g}_k(N_k-1)$ (more specifically, at most $K-1$ of them). Then N gets reduced by at most $K-1$. However, the desired column $\tilde{g}_k$ is non-sparse and is linearly independent of others, and so, L given by (17) remains sufficient.

In the case of $K^{'}$ very high (same) rate users with the same l_k's, the situation is slightly different. The $\tilde{\boldsymbol{g}}_k$'s now contain very few (p) non-zero elements. As soon as $K^{'} > p$, the rank of $\mathcal{T}_L(\boldsymbol{G}_N)$ drops, and the desired column $\tilde{\boldsymbol{g}}_1$ is not linearly independent of others. In this case, an instantaneous mixture of different users' channels is obtained. In a general, asynchronous, several rates case, however, the split-up approach remains robust from the identifiablity point of view.

The condition (**ii**) can be restated as the following dimensional requirement:

$$\mathrm{rank}\{\mathcal{T}_L(\boldsymbol{G}_N)\}+\mathrm{rank}\{\boldsymbol{T}_1^H\}\leqslant\mathrm{row}\{\mathcal{T}_L(\boldsymbol{G}_N)\}+1, \tag{18}$$

from where, under the irreducible channel and column reduced conditions,

$$L \geq \underline{L} = \left\lceil\frac{N-K+l_1MJ-1}{(PMJ)_{\mathrm{eff}}-K}\right\rceil, \tag{19}$$

where, l_1 is the channel length for user 1 in chip periods. If (19) holds, then condition (**ii**) is fulfilled w.p. 1, regardless of the N_k's, i.e., the $\mathrm{span}\{\boldsymbol{T}_1^H\}$ does not intersect with all shifted versions of $\boldsymbol{g}_k$'s, $\forall k \neq 1$, which further means that no confusion is possible between the channel of the user of interest and those of other users, whether the mixing is static (same orders) or dynamic (different channel lengths), with lengths measured in symbol periods.

The banded matrix of fig. 3 for a sub-user of a u_k rate user has a band of width P_k. The matrix $\boldsymbol{T}_1^H$ is still full column rank. If the channel length (in symbol periods) is not over-estimated, then there is no confusion possible between the u_k sub-users. Due to the zero-padded spreading sequences of length P, some symbol contributions will be zero for certain sub-users, k. This drops the rank in $\mathcal{T}_L(\boldsymbol{G})$. However, the effect is that of a reduced channel length and the zero columns can be conveniently considered as non-existant.

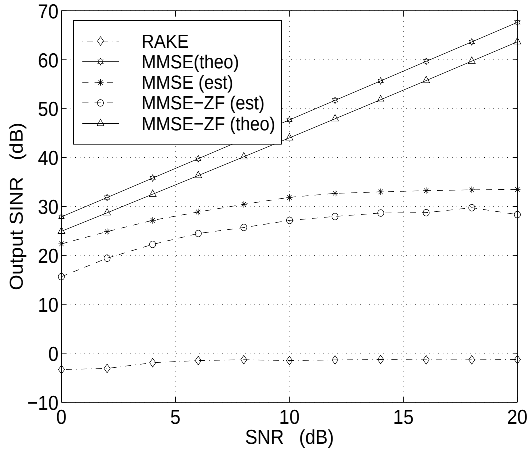

Figure 6. Output SINR performance of different receivers in near-far conditions for spreading factor, $P = 16$, and $K^{'} = 2$ multirate users, with $u_1 = 4,\ \ u_2 = 1$.

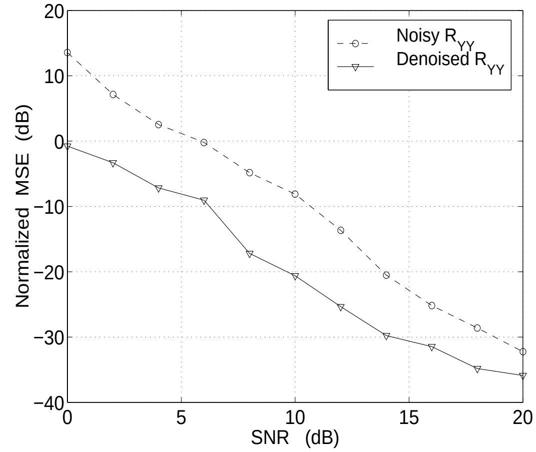

Figure 7. Normalized channel estimation MSE for the denoised and non-denoised $\boldsymbol{R}_{YY}$, for spreading factor, $P = 16$, and $K^{'} = 2$ multirate users, with $u_1 = 4,\ \ u_2 = 1$.

V. NUMERICAL EXAMPLES

We consider $K^{'} = 2$ asynchronous users in the system with a spreading factor of $P = 16$. User 1 is a $u_1 = 4$ times faster user in terms of its transmission rate. Hence the effective processing gain $P_1 = 4$. The user 1 is split into 4 parallel users with modified spreading sequences (padded with zeros as shown in fig. 1). This gives us $K = 5$ as the effective number of users. The propagation channel for both users is modeled as a FIR channel of order $l_k = 12,\ k = 1, 2$. The channel therefore introduces significant ISI for user 1's signal. The interfering user is 10 dB. stronger than the user of interest. An oversampling (multiple sensor) factor of $J = 1$ ($M = 1$) is assumed in these simulations.

Fig. 6 shows the performance of different receivers in terms of the output signal-to-interference-and-noise (SINR) ratios. An average over 50 Monte-Carlo runs is performed and 500 data samples are used in all cases for the estimation of the receivers.

Fig. 7 shows that the channel is estimated fairly accurately (normalized mean squared error [2] (NMSE) of the order of -20 dB at 10 dB. SNR) with 500 symbols from the rank-1 $\boldsymbol{R}_{ZZ}$ (see section IV). For comparison, channel estimated with non-denoised statistics has also been shown. Denoising is done to get a proper implementation of the algorithm in the noisy case (to ensure a distortionless response for the desired user) [2].

These figures show the results averaged over the two cases where the desired user is the (a) slow rate user, and (b) a sub-user of the faster rate one.

VI. CONCLUSIONS

A multirate DS-CDMA system was presented. It was shown that the faster (high transmission rate) users could be split up into a number of slow rate users with modified spreading sequences (zeros padded at the appropriate places). It was furthermore observed, that the identifiability conditions stay the same as in the case of a monorate system (common processing gain P for all users). Channels for different users can therefore be estimated blindly (upto a scalar phase factor) from the MMSE-ZF receiver algorithm. For a given processing window (L), the actual number of physical users in the system then depends on the rates of different users. The actual capacity of the system in terms of physical users can therefore be rather low. Another interesting observation is that the same the number of data is available per transmission block for all effective users, rendering the estimation performance equal for all users, irrespective of their rates.

[2]NMSE$= E\frac{\|\boldsymbol{h}_1 - \hat{\boldsymbol{h}}_1\|^2}{\|\boldsymbol{h}_1\|^2} = \frac{1}{L}\sum_{i=1}^{L} \frac{\|\boldsymbol{h}_1 - \hat{\boldsymbol{h}}_1^{(i)}\|^2}{\|\boldsymbol{h}_1\|^2}$

VII. REFERENCES

[1] European Telecommunications Standards Institute, *Concept Group Alpha-Wideband DS-CDMA*, December 1997.

[2] I. Ghauri and D. T. M. Slock, "Blind projection receiver for asynchonous CDMA in multipath channels," *Annals of Telecommunications*, September 1999. to appear.

[3] C. Schlegel, S. Roy, P. Alexander, and Z. Xiang, "Multiuser projection receivers," *IEEE J. on Selected Areas in Communications*, vol. 14, pp. 1610–1618, October 1996.

[4] M. Saquib, R. Yates, and N. B. Mandayam, "Decorrelating detectors for a dual rate synchronous DS-CDMA channel," *Special issue on Interference in Mobile Wireless Systems*, 1997.

[5] D. T. M. Slock, "Blind joint equalization of multiple synchronous mobile users using oversampling and/or multiple antennas," in *Proc. 28th Asilomar Conf. on Signals, Systems & Computers*, (Pacific Grove, CA), November 1994.

[6] D. H. Johnson and D. E. Dudgeon, *Array Signal Processing - Concepts and Techniques*. Englewood Cliffs, NJ: Prentice Hall, 1993.

[7] A. Duel-Hallen, J. Holtzman, and Z. Zvonar, "Multi-user detection for CDMA systems," *IEEE Personal Communications Magazine*, pp. 46–58, April 1995.